JGR Atmospheres

RESEARCH ARTICLE
10.1029/2020JD033554

Aerosol Climatology Over South and Southeast Asia: Aerosol Types, Vertical Profile, and Source Fields

Tirthankar Banerjee[1,2], A. S. Shitole[1], Alaa Mhawish[1], A. Anand[3], R. Ranjan[1,2], Md F. Khan[4], T. Srithawirat[5], Mohd T. Latif[6], and R. K. Mall[1,2]

[1]Institute of Environment and Sustainable Development, Banaras Hindu University, Varanasi, India, [2]DST-Mahamana Centre of Excellence in Climate Change Research, Banaras Hindu University, Varanasi, India, [3]Department of Botany, Banaras Hindu University, Varanasi, India, [4]Department of Chemistry, Faculty of Science, University of Malaya, Kuala Lumpur, Malaysia, [5]Department of Environmental Science, Pibulsongkram Rajabhat University, Phitsanulok, Thailand, [6]Department of Earth Sciences and Environment, Universiti Kebangsaan Malaysia, Bangi, Malaysia

Abstract Aerosol climatology during typical haze dominating period over South and Southeast Asia was explored using several Earth-Observing A-Train satellite products retrieved in between 2010 and 2020. Comparatively high aerosol optical depth (AOD) with dominance of fine and UV-absorbing aerosols are noted across the Indo-Gangetic plain, South Asia (IGP; AOD: 0.58; UVAI: 0.74) against weak UV-absorbing fine aerosols over Southeast Asia (SEA; AOD: 0.26; UVAI: 0.07). Among inland IGP sites, decadal mean AOD resembles in Lahore (0.72 ± 0.45), Delhi (0.81 ± 0.46), Kanpur (0.84 ± 0.42), and Varanasi (0.78 ± 0.45); all exhibiting bimodal AOD distribution with a first peak in early November followed by a second in early January. In contrast, except mainland site Chiang Mai, all SEA maritime cities resemble in having typical September-October AOD peak, with the presence of fine and UV-neutral aerosols. Urban hotspots across IGP and SEA (except Dhaka, Chiang Mai) denote a spatially consistent minor increasing trend in AOD ($0.2–1.8 \times 10^{-2}$ year^{-1}) while increase in UVAI is more prominent over upper IGP. Dust aerosols dominate only in Karachi (46%) against strong UV-absorbing smoke aerosols over rest of the IGP (71–91%), and UV-neutral smoke aerosols across SEA (84–92%). Vertical stratification of aerosol types is noted across IGP as in lower atmosphere (<4 km) polluted dust/urban aerosols remain abundant, with gradual decrease in dust aerosols from upper to lower IGP and consequent increase in smoke aerosols. At upper atmosphere (>4 km), however, dust aerosols clearly dominate. Over SEA, smoke are the most abundant aerosols across the atmospheric column followed by polluted dust. No evidence of intracontinental transport of aerosols from IGP to Southeast Asia or vice versa is, however, noted.

Plain Language Summary Aerosol climatology during typical haze dominating period over two global aerosol hotspots: South and Southeast Asia was explored using several satellite-based aerosol optical properties retrieved using Earth Observing A-Train satellites (Aqua, Aura, CALIPSO). Comparatively high aerosol optical depth with dominance of fine and absorbing aerosol are noted across the Indo-Gangetic plain, South Asia against weak absorbing fine particles over Southeast Asia. Presence of strong absorbing aerosol over Indo-Gangetic plain may have greater implications on regional climate. We note absorbing dust aerosols only over Karachi against strong absorbing smoke aerosols over Lahore, Delhi, Kanpur, Varanasi, and Dhaka, and UV-neutral smoke aerosols over Singapore, Penang, and Kuala Lumpur. Vertical stratification of aerosol types is also noted across IGP as in lower atmosphere (<4km) polluted dust/ polluted urban aerosol remains abundant, with gradual decrease in dust aerosols from upper to lower IGP and consequent increase in smoke aerosols. No evidence in intracontinental transport of smoke aerosols is found, as biomass burning emissions over upper IGP, Kalimantan, and Sumatra primarily modulating climatology of regional aerosols.

Key Points:

- Smoke aerosols are more UV-absorbing across South Asia compared to Southeast Asia
- Vertical stratification of aerosols is prominent over IGP as urban aerosols and smoke dominate at low altitude while mineral dust at high altitude
- Smoke and urban aerosols are abundant across the atmospheric column over SEA

Supporting Information:

- Supporting Information S1

Correspondence to:

T. Banerjee,
tb.iesd@bhu.ac.in;
tirthankaronline@gmail.com

Citation:

Banerjee, T., Shitole, A. S., Mhawish, A., Anand, A., Ranjan, R., Khan, M. F., et al. (2021). Aerosol climatology over South and Southeast Asia: Aerosol types, vertical profile, and source fields. *Journal of Geophysical Research: Atmospheres*, *126*, e2020JD033554. https://doi.org/10.1029/2020JD033554

Received 19 JUL 2020
Accepted 22 FEB 2021

Author Contributions:

Conceptualization: Tirthankar Banerjee, Alaa Mhawish
Formal analysis: A. S. Shitole, Alaa Mhawish, A. Anand, R. Ranjan
Funding acquisition: Tirthankar Banerjee, R. K. Mall
Investigation: Tirthankar Banerjee, A. S. Shitole, A. Anand, R. Ranjan
Methodology: Tirthankar Banerjee, Alaa Mhawish
Project Administration: Tirthankar Banerjee
Resources: Tirthankar Banerjee, Md F. Khan, T. Srithawirat, Mohd T. Latif
Software: Tirthankar Banerjee
Supervision: Tirthankar Banerjee
Validation: Alaa Mhawish
Writing – original draft: Tirthankar Banerjee

1. Introduction

Among many globally recognized aerosol hotspots, both South and Southeast Asia have been studied and documented most extensively (Huijnen et al., 2016; Singh et al., 2017a, 2017b; Vadrevu et al., 2019; Yin et al., 2019); owing to their common vulnerabilities to possible implications of aerosols on regional climate (Ramanathan et al., 2001), atmospheric chemistry (Duncan et al., 2003), hydrological cycle (Bollasina et al., 2011; Vinoj et al., 2014), fragile ecosystem (Sonkar et al., 2019; Turetsky et al., 2015; Yanhong

Writing – review & editing: Tirthankar Banerjee, Md F. Khan, T. Srithawirat, Mohd T. Latif, R. K. Mall

et al., 1996), and perturbations to economically sensitive population (Quah & Johnston, 2001). Together, these two regions account for nearly 33% of world population with 25% of global fine particulate and 28% of black carbon emissions (in 2010), considerable proportion of which originate from the forest and other biomass burning emissions (Klimont et al., 2017). The growing demand for energy, intensive land-use-based urbanization and industrialization, deforestation related to agricultural expansion, limited and inefficient public transport system, indiscriminate waste/refuse burning; all these lead to massive emissions of aerosols and their precursors. Exposure to such airborne particulates has been vowed to cause severe negative health impacts and millions of premature deaths, especially over these two geographical regions (Sahani et al., 2014; Singh et al., 2021a).

Beside conventional sources of aerosols (like industrial and vehicular emissions), Southeast Asia (SEA) experiences widespread and ubiquitous emissions from forest fire, peatland combustion, and slash and burn agricultural activities (Latif et al., 2018; Nguyen et al., 2019; Vadrevu et al., 2019). These fires are often sufficiently intense and spread across (Vadrevu et al., 2014), frequently intensified by El Niño mediated hydrological drought and pattern in Indian Ocean Dipole (Field et al., 2009). This has been a common scenario from last half a decade and has been accounted for releasing huge amounts of terrestrially stored carbon, smoke, and other primary and secondary aerosols (Cohen, 2014; Huijnen et al., 2016; Stockwell et al., 2016). Characteristically, two typical trends in fire occurrence prevail over SEA. Mainland countries like Thailand, Myanmar, Cambodia, and Vietnam experience peak in fire density and associated poor air quality during March-April with a second peak in October; whereas the maritime countries (Indonesia, Malaysia, Singapore, Philippines) experience the same during September-October (Nguyen et al., 2019; Vadrevu et al., 2019). Indeed, fire strength and emission vary with space, biomass type, topography, and climate but in general, carbonaceous smoke particle, secondary inorganic and organic dominate the aerosol constituents (Huijnen et al., 2016; Latif et al., 2018).

In contrast, over South Asia, the Indo-Gangetic plain (IGP) bears the highest burden of aerosols (Dey & Di Girolamo, 2011; Kumar et al., 2018; Mhawish et al., 2020); aerosols which are highly diverse (Gautam et al., 2011; Jethva et al., 2005; Mhawish et al., 2017, 2019), dynamic (Dey et al., 2008; Rajput & Sarin, 2014; Singh et al., 2017a) with signature of multiple emissions sources (Chakraborty et al., 2015; Singh et al, 2017b, 2021b). Both observational (Gautam et al., 2011; Jethva et al., 2019; Singh et al., 2018; Vinjamuri et al., 2020) and model simulations (Henriksson et al., 2011; Ojha et al., 2020) indicate the predominance of mineral dust during premonsoon while biomass burning, waste/refuse incineration and residential emissions essentially contribute in postmonsoon and winter months. Also, there are several reports of consistent increase in surface $PM_{2.5}$ (Shi et al., 2018) and columnar aerosol loading over IGP, a trend varying from 0.007 $years^{-1}$ over northern India (Krishna Moorthy et al., 2013) to 0.01–0.04 $years^{-1}$ over IGP (Dey & Di Girolamo, 2011), with a recent estimate by Kumar et al. (2018) as 0.002 $years^{-1}$. Notably, the rate of increase is more pronounced during October to February months (Kumar et al., 2018; Srivastava, 2017) with greater incidence of hazy days (Singh et al., 2021a; Thomas et al., 2019) and consequent atmospheric warming, frequently associated to emissions from indiscriminate biomass burning and anthropogenic sources.

Yet our understanding on the sectoral emissions of aerosols, its nature and atmospheric chemistry, transport and vertical distributions are severely limited; constrained especially by the absence of coordinated ground-based observations, and heterogeneity in emissions sources and strengths. Here, we have explored the nature of aerosols and its spatial-temporal-vertical distributions across two geographical regions, with specific emphasis on urban pollution hotspots, using multiple coordinated earth observation satellite products, retrieved in between September 2010 and February 2020. However, instead of analyzing year-long variations we intend to focus only on haze dominated period. We took advantages of multiple satellite-based aerosols products; established initially the spatial signature of aerosol loading, its optical and microphysical properties, followed by aerosol trend, distinguished prevailing aerosols constrained by their size and light-absorbing properties, explored vertical gradient in aerosol extinction and concluded by recognizing potential emission source fields. Our analysis has limitation in exempting surface $PM_{2.5}$ measurements but have broader implications in recognizing nature of aerosols during hazy days, in improving aerosol-particulate modeling and in epidemiological studies.

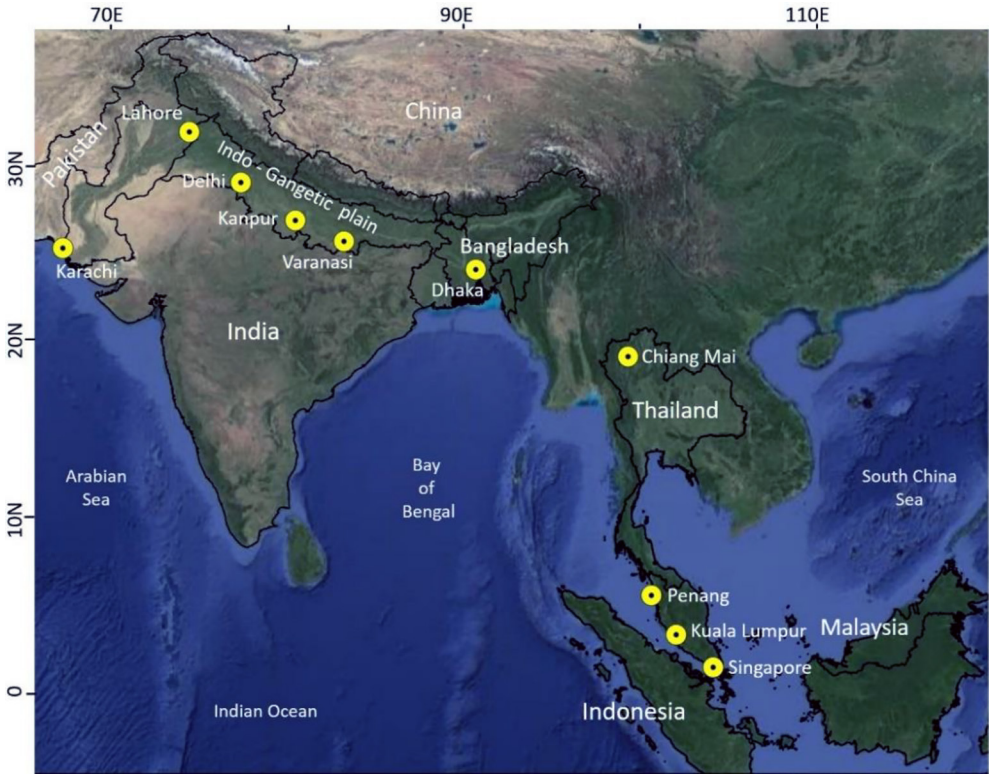

Figure 1. Geographical location of the study domain and spatial distribution of selected sites across South and Southeast Asia. *Note*: To compare geospatial means of aerosol properties, only the geographical regions of IGP (for South Asia) and Thailand, Malaysia, Singapore, and Indonesia (for Southeast Asia) were considered. Yellow dot indicates urban hotspots considered for analysis. IGP, Indo-Gangetic plain.

2. Data and Experimental Methods

2.1. Site Description

Geospatial analysis was done initially for two large geographical regions: South Asia and Southeast Asia considering every single pixel, followed by 10 individual sites located across two regions (Figure 1). Here, IGP was considered to represent South Asia as it possesses the maximum burden of particulate loading (Dey & Di Girolamo, 2011; Kumar et al., 2018) with presence of highly diverse and dynamic aerosols (Dey et al., 2008; Gautam et al., 2011; Mhawish et al., 2017) having considerable spatiotemporal variations (Jethva et al., 2005; Vinjamuri et al., 2020). In comparison, geographical regions of Thailand, Malaysia, Singapore, and Indonesia were earmarked as Southeast Asia.

Individual sites were selected considering their representativeness of broad geography, predominating aerosol types and sources, prevailing meteorology, and population count. A very brief description of individual sites is included here while detailed discussions may be found in Singh et al. (2017b), Kumar et al. (2018), and reference therein. Karachi (24.95°N, 67.13°E), is a typical coastal city in southeast Pakistan with industrial and vehicular emissions as predominating sources of aerosols, periodically influenced by deserts dust and marine aerosols (Mansha et al., 2012). Lahore (31.48°N, 74.26°E) located at northern Pakistan experiences seasonal reversal of emission sources with vehicular and industrial emissions, biomass burning and transported dust contribute to local particulates (Stone et al., 2010). New Delhi (28.63°N, 77.17°E), having one of the world's poorest air quality experiences variety of aerosol sources and mix aerosol types; with abundance of dust during the premonsoon and fine aerosols from biomass burning, vehicular and industrial sources (Jain et al., 2020). Kanpur (26.51°N, 80.23°E), an industrial city in central IGP experiences seasonal variations in aerosol types linked to biomass and refuse burning emissions, with dominating proportions of carbonaceous and sulfate aerosols (Chakraborty et al., 2015). Varanasi (25.31°N, 82.97°E), reported to have the highest columnar aerosol loading among the cities in IGP (Kumar et al., 2018); have aerosols mostly of

secondary in nature with contribution from biomass/waste burning, crustal resuspensions, and residential emission sources (Murari et al., 2020; Singh et al., 2021b). Fine absorbing aerosols mainly prevail in Dhaka (23.72°N, 90.39°E), with sources like vehicular emissions, household energy practices and emissions from brick kilns (Begum et al., 2004). Among the cities located in Southeast Asia, Chiang Mai (18.81°N, 98.98°E) is in northwest Thailand influenced mainly by forest fires and biomass burning aerosols (Guatam et al., 2013). Penang (5.35°N, 100.30°E) located in the northwest coast of Peninsular Malaysia and primarily is an industrial hub. Singapore (1.29°N, 103.78°E), a highly industrialized global megacity, is affected by fossil fuel emissions from cars, petrochemical industries, and ship emissions with periodic influence from marine and biomass burning aerosols (Nguyen et al., 2019). Kuala Lumpur (3.13°N, 101.68°E), situated in the west coast of the Malaysian Peninsula; essentially have secondary and biomass burning aerosols, with intermittent contribution from road dust and marine aerosols (Sulong et al., 2017).

2.2. Satellite-Based Observations

This study integrates observation from several coordinated Earth Observing System (EOS) satellites, including the Afternoon Constellation (A-Train) satellites like Aqua and Aura, and C-Train satellite like CALIPSO (Cloud-Aerosol Lidar and Infrared Pathfinder Satellite Observation). All these coordinated group of polar satellites have near synchronous orbit crossing within minutes of each other thereby, providing near-simultaneous observation of both spatial, temporal, and vertical distribution of aerosols. To create three-dimensional aerosol climatology of atmospheric haze over South and Southeast Asia; we followed Moderate Resolution Imaging Spectroradiometer (MODIS, Aqua) and the Ozone Monitoring Instrument (OMI, Aura) to assess spatial nature of aerosol optical and microphysical properties while Cloud-Aerosol Lidar with Orthogonal Polarization (CALIOP, CALIPSO) was used to distinguish the vertical distribution of aerosols.

All the satellite data were retrieved for a period of 10 years (September 2010 to February 2020, all inclusive) exclusively for the haze dominating period over South and Southeast Asia. However, it should be noted that atmospheric haze was not defined here on a daily basis constrain by the fact that we did not account for ground-level $PM_{2.5}$ concentration and visibility data, and CALIPSO has a revisit period in each 16 days. Across IGP, there are evidences of greater incidence of hazy days with very high aerosol concentration during October to November (Thomas et al., 2019), influenced mainly by the burning of agricultural residues (Jethva et al., 2019; Singh et al., 2018). From December to February, haze episodes are mostly accompanied with the burning of biomass/waste/refuse, that are frequently practiced for residential heating and cooking purposes (Singh et al., 2021b). In a separate manuscript based on ground-based $PM_{2.5}$ observation in Varanasi, we have noted 67% of monitoring days (in between 2009 and 2016) were haze days, most frequently (>80%) from October to February months (Singh et al., 2021a). In contrast, over Southeast Asia, haze episodes are most frequent during southwest monsoon (September-October) while the intermonsoon (October-November) and northeast monsoon (December-March) also pose haze days with high aerosol concentration with dominance of smoke aerosols (Nguyen et al., 2019; Sulong et al., 2017). Therefore, in each year, October to February months over South Asia, and September to January over Southeast Asia were selectively considered as haze dominating period, and followed for satellite retrievals and geospatial analysis.

2.2.1. Aqua-MODIS AOD and AE

For this analysis, we relied on MODIS onboard EOS Aqua satellite for retrieval of aerosol optical properties. The MODIS sensor measures the earth and atmospheric radiance on a systematic manner, and provides retrievals in 36 spectral bands from 0.415 to 14.235 μm. MODIS AOD (aerosol optical depth) retrievals have been validated widely both on global (Sayer et al., 2019) and regional scale (Bilal & Nichol, 2015), and over IGP (Mhawish et al., 2017). Three independent MODIS aerosol retrieval algorithms are in operation viz. Dark Target (DT) for dark or vegetated surfaces, DT over ocean, and Deep Blue (DB) for universal land surface. Recently, Lyapustin et al. (2011) introduced the Multiangle Implementation of Atmospheric Correction (MAIAC), a new generic aerosol algorithm which has been proved to be effective in identifying fine aerosols and emission sources over varying land surfaces (Mhawish et al., 2019).

Aqua MODIS (C6.1) aerosol product was used to retrieve aerosol optical and microphysical properties. The combined DT and DB AOD product was used to retrieve aerosol optical depth (AOD at 10-km resolution) considering its capability to retrieve aerosols over varied land surfaces. Only highest quality (QA > 2) AOD

data were retrieved from September 2010 to February 2020 (all inclusive) to assess the spatiotemporal variations of aerosol loading. To retrieve information on microphysical properties of aerosols, Aqua MODIS (C6.1) DB angstrom exponent (AE at 10-km resolution) with recommended quality flag (QA > 2) was used as a qualitative indicator of aerosol size.

2.2.2. Aura-OMI UVAI and AAOD

To distinguish UV-absorbing aerosols (e.g., absorbing part of carbonaceous aerosols and desert dusts) against scattering aerosols (sulphate aerosols), we retrieved UV-Aerosol Index (UVAI) from OMI sensor onboard Aura satellite (Herman et al., 1997; Torres et al., 2007). The UVAI is a function of aerosol optical depth, aerosol absorption, and layer height; and a proven semiquantitative parameter that has been widely used to trace distribution of absorbing aerosols (Jethva et al., 2018, 2019; Singh et al., 2018;Zhang et al., 2017). To retrieve UVAI, we considered spectral measurements at 354 and 388 nm using OMI near-UV aerosol retrieval algorithm (OMAERUVG, V3, Level 2G data) retrieved at 0.25° × 0.25° resolution. A detail discussion on OMAERUV algorithm and its uncertainties is included in Jethva et al. (2014) and Ahn et al. (2014). Besides UVAI, we also retrieved and processed absorbing aerosol optical depth (AAOD) from Aura-OMI sensor using same algorithm with associated quality flag (1). AAOD was used to denote nonscattering part of AOD which also serves as a proxy for absorbing aerosols (Ahn et al., 2014; Zhang et al., 2017).

2.2.3. CALIPSO-CALIOP Aerosol Extinction

Vertical distribution of aerosols serves categorical information on potential transport, chemistry, interaction with cloud and radiation, and its removal mechanism (Bourgeois et al., 2018; Winker et al., 2009). Aerosol attenuated backscatter profiles over each station (1° × 1°) was retrieved from space borne active lidar CALIOP onboard CALIPSO satellite. The CALIOP is a dual-wavelength (532 and 1,064 nm) elastic polarization lidar that retrieves aerosol backscatter profiles at 30–60 m vertical resolutions with detection sensitivity of 0.01–0.07 km^{-1} (Winker et al., 2009). Recent improvements on CALIOP V4 Level 2, uncertainties and global validation of CALIOP AOD against ground observation are reported by Kim et al. (2018). For this research, aerosol extinction coefficients at 532 nm were retrieved using latest and improved CALIPSO version 4.20 (V4) Level 2 5-km aerosol profiles. Individual aerosol types were classified based on Kim et al. (2018) and only nonnegative aerosol extinctions with designated quality flags (0, 1, 18, or 16) and cloud-aerosol discrimination criterion (CAD ≤ −20; ≠−101) were considered.

2.3. ERA-Interim Data

Wind vector profile at 10 m a.g.l. across the study domain was obtained from the European Centre for Medium-range Weather Forecasts (ECMWF) ReAnalysis-Interim (ERA-Interim) data set. The ECMWF reanalysis data are based on several EOS and weather prediction models, and provide better accuracy and resolution compared to other contemporary data set. Vector wind was retrieved at 0.25° × 0.25° horizontal resolution only for a single representing year (September 2018 to February 2019) and monthly means were plotted using Grid Analysis and Display System (GRADS).

2.4. Air Mass Back Trajectories

Five-day isentropic air mass back trajectories for all the sites across IGP and SEA were plotted by Hybrid Single Particle Lagrangian Trajectory (HYSPLIT) model. We have used GDAS (1° × 1°) archived data set to run HYSPLIT, averaged from September 2018 to February 2020. Constraining the prevailing boundary layer height, backward trajectories were plotted at 500 and 1,500 m for sites over IGP (Murari et al., 2017), and 1,500, 1,900, and 2,300 m for sites over Southeast Asia (McGrath-Spangler & Denning, 2013). Concentration weighted trajectories (CWTs) were drawn using GIS-based TrajStat software (Wang et al., 2009) to recognize potential aerosol source fields.

2.5. Data Processing

Spatial variations in aerosol loading and aerosol types across South and Southeast Asia were investigated during haze dominated period. We took advantages of a set of robust satellite-retrieved data set including

AAOD, AOD, UVAI, and AE to classify existing aerosol types. Selection of UVAI and AE thresholds is motivated by the ability of OMI OMAERUV product UVAI to accurately distinguish absorbing (+UVAI) and scattering aerosols (−UVAI) while MODIS DB product AE was considered as a proxy for aerosol size. Spatial dominance of fine absorbing aerosols (like smoke aerosols) was traced by the prevalence of high (+) UVAI, AAOD with a corresponding high AE value (>1.2).

We also tried multidimensional clustering analysis to ascertain existing aerosol types over individual sites across two geographical regions. A 1° × 1° spatial grid centered over each site, as discussed in Section 2.1; is uniformly selected to retrieve daily area-weighted mean of AOD, AE, AAOD, and UVAI. They were first used to recognize any reiterating pattern that exist in daily variations of the parameters in between the cities, before being subject to multiyear trend analysis using nonparametric statistical test. A standard Mann-Kendall (M-K) test was used to estimate the monotonic trend in aerosol time series following Kumar et al. (2018) and Li et al. (2014).

Identification of prevailing aerosol types is often challenging and many researchers have explored ways to identify aerosol types using either sensors with diverse range of spectrum or by using multiple satellite sensors (Jeong & Li, 2005; Kim et al., 2007; Lee et al., 2010; Penning de Vries et al., 2015). In order to classify aerosol types, we followed defined protocol of aerosol type classification by Penning de Vries et al. (2015) and Vinjamuri et al. (2020). Classification of aerosol types was done following UV radiation absorptivity of aerosols and effective particle size. Here, we classified aerosol absorption in UV range as scattering (S), neutral (N), and absorbing (A); considering UVAI threshold as a semiquantitative indicator of aerosol absorption (Zhang et al., 2017). To classify aerosol size, we considered AE over FMF (fine mode fraction). Although, FMF, defined as fine-mode AOD to total AOD, is a quantitative parameter; it is not included in MODIS DB algorithm product. Therefore, FMF is unable to provide reliable estimation of aerosol size over bright surfaces like in upper IGP. Besides, AE is widely considered to constrain particle size (Mhawish et al., 2017; Penning de Vries et al., 2015; Sayer et al., 2019). Briefly, three aerosol types according to its sizes e.g., coarse (AE < 0.7), mixed (0.7 < AE < 1.2) and fine aerosols (AE > 1.2); and three types according to their UV-absorption potential e.g., scattering (UVAI < −0.5), neutral (−0.5 < UVAI < 0.25) and absorbing aerosols (UVAI > 0.25) were defined with a total of nine independent aerosol subtypes.

To investigate vertical distribution of aerosols, CALIOP attenuated backscatter profiles fall within each selected grid of 1° × 1° for each city was considered. We did not segregate day and night profiles as diurnal variation in aerosols was not intended. A total of 431332 CALIOP lidar profiles were considered spanning from a range of 2,604 (in Singapore) to 97,243 (in Lahore) profiles for each city. Cloudy profiles were removed using the Cloud-Aerosol Discrimination score (inclusive of -100 to -20). At each vertical bin, respective extinction coefficients of individual aerosol subtypes were compared against total extinction including the scenarios marked as "0" when null contribution of a particular aerosol type was noted.

3. Results and Discussion

3.1. Spatial Distribution of Aerosols

Spatial distributions of aerosols during typical haze dominating period over South (October-February) and Southeast Asia (September-January) are included in Figure 2 while intraperiodical averages are in Table S1 (in supporting information). Clearly, the Indo-Gangetic plain (IGP) depicts the highest columnar aerosol loading (AOD) with area-weighted spatial mean of 0.58 against 0.26 over Southeast Asia (SEA). For the IGP, the spatial mean of AOD during haze is slightly high compared to the reported annual mean of 0.50 from 2006 to 2015 (Kumar et al., 2018) and from 2008 to 2017 (0.55; Vinjamuri et al., 2020). Significant spatial gradient in aerosol loading is also evident with comparatively high AOD over central to lower parts of IGP. This is also true over Southeast Asia as eastern Indonesia, southern part of Malaysia, and west Kalimantan (Indonesian Borneo) recorded higher aerosol loading compared to rest of the region.

Across two geographical regions, spatial variations in AE are less stringent with geospatial average ranging from 1.39 (IGP) to 1.49 (SEA) indicating dominance of fine particulates. Figure 2 also indicates that the distribution of fine particulates is not robust and does not correspond well to the spatial variations in columnar aerosol loading. In terms of UV-absorbing potential of prevailing aerosols, geographical distinctions between IGP and SEA are clearly evident. The IGP is accompanied with more UV-absorbing aerosols (spatial

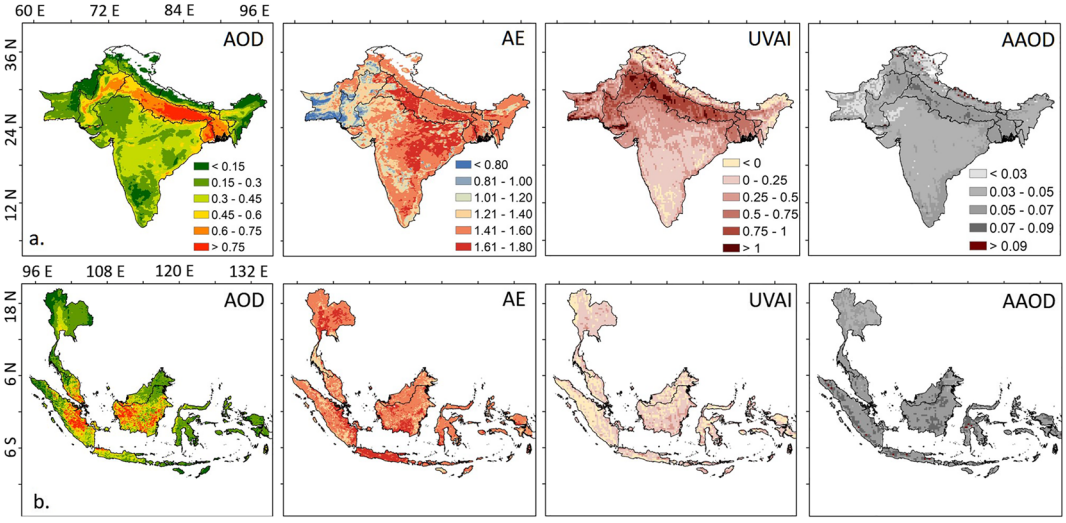

Figure 2. Spatiotemporal nature of aerosols across (a) South and (b) Southeast Asia in between 2010 and 2020.

mean: 0.74), especially over the upper IGP (>0.75), whereas no such dominance in absorbing aerosols is noted over SEA (spatial mean: 0.07). Presence of absorbing aerosols over upper part of the IGP overlaps well with the region that accounts for the emissions of carbonaceous aerosols from burning of crop residues (Jethva et al., 2019; Singh et al., 2018; Vinjamuri et al., 2020). Spatial variations in AAOD, a reliable indicator of absorbing aerosols, are not evident across IGP and SEA as both the regions account for a low spatial mean (0.06) during haze dominated period.

We also account for the intraperiodic variations in spatial means (Figure S1 and Table S1); considering two distinct seasons i.e., postmonsoon (ON) and winter (DJF) over IGP, and southwest monsoon (SO) and inter and northeast monsoon (NDJ) over SEA. Although the IGP suffers greater accumulation of smoke particles during October to February months, the dominant sources are reported to be biomass burning emissions during ON (Jethva et al., 2019; Singh et al., 2018) while emissions from waste/refuse and biomass burning contributes mainly during DJF (Singh et al., 2021b). Here, geospatial mean AOD over IGP remains similar during ON and DJF (0.58) but aerosols that prevail over upper IGP during ON seems to be transported toward central to lower IGP by westerly wind (Figure S1a). In contrast, over SEA, spatial mean AOD is considerably high during southwest monsoon (SO: 0.35; NDJ: 0.18); particularly over east Indonesia and west Kalimantan (AOD > 0.75). High AOD during SO months over Indonesia corresponds well with AOD retrieved during extreme biomass burning events (AOD: 0.80; Vadrevu et al., 2014). The continental SEA, especially northern Thailand, Myanmar, and Vietnam usually experience the highest biomass burning events, highest AOD and corresponding haze during March-April-May months while over Malaysia, Indonesia, and Singapore, maximum AOD prevail during September to October months (Nguyen et al., 2019). In contrast, temporal variations in particulate size (AE; IGP: 1.33–1.43; SEA: 1.48–1.51) are insignificant, although there is definite increase in UV-absorbing potential during high biomass burning episodes both over IGP (ON: 0.842, DJF: 0.667) and SEA (SO: 0.073; NDJ: 0.055). Similarly, AAOD increases slightly during early haze period, both over IGP and SEA; coinciding well with the region that typically experiences high biomass burning events. Overall, spatial distribution of multiple satellite-retrieved aerosols indicates possible contribution of regional biomass burning emissions in regulating air quality which was further explored in the following section.

3.2. Characteristics of Aerosols Over Urban Hotspots

Variations in aerosol loading (AOD), optical (AAOD and UVAI), and microphysical properties (AE) of aerosols for individual cities across IGP and SEA for the entire haze dominating period are plotted in Figure 3 with descriptive statistics included in Table S2. Clearly, cities across IGP have high and distinct variations in AOD contrast to SEA cities. However, only exception to this is in Karachi (0.29 ± 0.15) where a low AOD

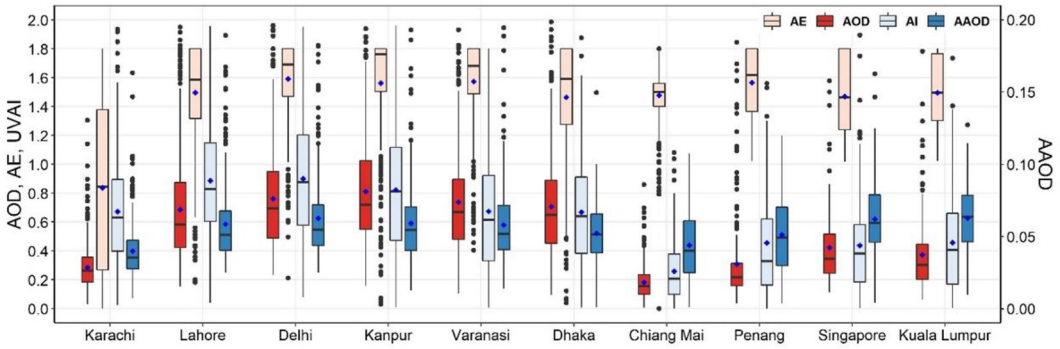

Figure 3. Variations in aerosol properties (AOD, UVAI, AE and AAOD) during haze dominating period in different cities across South and Southeast Asia from 2010 to 2020. AOD, aerosol optical depth; UVAI, UV-Aerosol Index; AE, angstrom exponent; AAOD, absorbing aerosol optical depth.

(±SD) with mixed (AE: 0.84 ± 0.58) and moderately absorbing aerosols (UVAI: 0.67 ± 0.37) prevails. Besides local dust aerosols, abundance of coarse particles over Karachi is possibly due to the hygroscopic growth of particles influenced by intrusion of moisture-laden marine aerosols from Arabian Sea (Bilal et al., 2016). To depict temporal variations in aerosol properties, daily time series of satellite retrievals averaged over 2010 to 2020 are included in Figures 4 and 5. Indeed, temporal variations in Karachi are insignificant except slight increase in particle size and absorbing aerosols during mid-November to the end of December (Figure 4).

As we move into inner continent toward northern Pakistan and India, influence of marine aerosols gradually diminishes, resulting dominance of fine aerosols with identical trend reciprocating over continental cities across IGP. Indeed, decadal mean AOD resembles in Lahore (0.72 ± 0.45), Delhi (0.81 ± 0.46), Kanpur (0.84 ± 0.42), and Varanasi (0.78 ± 0.45); with bimodal distribution in AOD having the first peak in early November followed by a second in early January. Even the distribution of AE as a proxy for fine particulates' abundance yield interesting features (Figure 4). All the four mainland sites denote extreme AE values (mean AE > 1.5) with high median (1.59–1.76) and least SD (±0.3), having evidence of exclusive dominance of fine particulates. However, an influx of coarse aerosols during late November to early December may also be noted, more distinctively over the cities in upper IGP (like in Lahore and Delhi) before dissipating over the central parts (as in Kanpur), and completely eliminating over Varanasi. Possible explanation to this may be the influence of dust aerosols, particularly over the upper IGP which is comparatively dry and dust dominated region in contrast to the central/lower IGP. Besides, this also indicate the convergence of two distinct seasons, one postmonsoon (ON) with single abundant source of agriculture residue burning emissions (Jethva et al., 2019; Singh et al., 2018) and winter (DJF) having many associated sources, however, being largely influenced by local meteorology, boundary layer in particular (Murari et al., 2017; Ojha et al., 2020). Predominance of UV-absorbing aerosols are also apparent in all the continental cities, with mean UVAI varying from 0.7 (Varanasi, Kanpur; SD: ±0.6) to 1.0 (Lahore, Delhi; SD: ±0.7). Clearly, peaks in UVAI during early to mid-November (UVAI > 1.3) with corresponding increase in AAOD (AAOD > 0.08; AE > 1.2) bear the signature of smoke aerosols. This has also been reported by Vinjamuri et al. (2020) using CALIPSO-based aerosol extinction coefficient over upper IGP. In contrast, AOD time series in Dhaka did not exhibit any early November peak exemplifying none contribution from agriculture residue burning emissions transported from the upper IGP. However, existing particles do pose characteristic signature of smoke aerosols with small particle size (AE: 1.46 ± 0.40) and high UV-absorption potential (UVAI: 0.59 ± 0.45).

Over SEA, distribution of aerosol loading and aerosol type in different urban hotspots has its own character (Figure 5). Chiang Mai in northern Thailand experiences minimum aerosol loading (0.18) and a modest temporal variation (±0.12) having complete dominance of fine (AE: 1.48 ± 0.20) and UV-neutral aerosols (UVAI: −0.02 ± 0.35). This is especially because continental SEA like Thailand experiences minimum biomass burning and haze events during September compared to March to May months (Nguyen et al., 2019). Rest of the SEA sites exhibit similar trend in aerosol loading with initial peak during September (AOD ~ 0.8) and consequent decrease; while overall mean varying from 0.31 (Penang) to 0.49 (Singapore). A similar trend in AOD time series is also reported by Nguyen et al. (2019). Intraperiodic variations in AOD and other

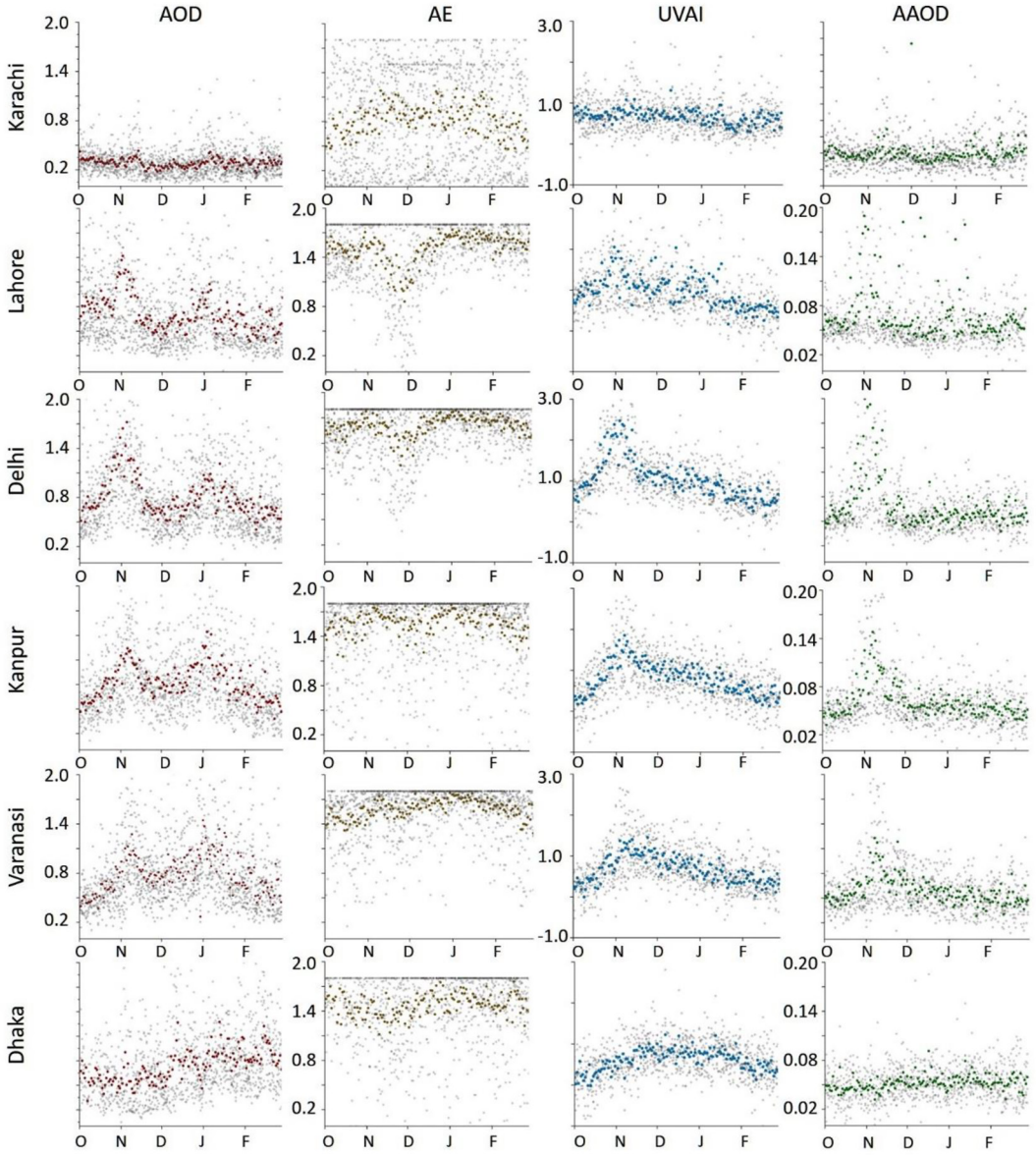

Figure 4. Time series of aerosol optical and microphysical properties in different urban hotspots across IGP. *Note*: Gray dots indicate daily retrievals while means averaged over 2010–2020 is indicated in color dot. To manage a similar scale for intercomparison, <2% of extreme observations were excluded. All the individual parameter bears identical scale (O, October; N, November; D, December; J, January; F, February). IGP, Indo-Gangetic plain.

aerosol properties also indicates a decline in aerosol loading post-October (Table S3) but variations in AE, UVAI, and AAOD are less significant indicating predominance of haze/smoke aerosols throughout the period, although with varying intensities. Clearly the existing aerosols are fine (AE: 1.47–1.57) with minimum SD (SD $\pm$ 0.2), and UV-neutral (UVAI: 0.07–0.17) with few event-specific influxes of scattering aerosols, may be of marine origin. Overall, feature that distinct aerosols over these two geographical regions is UV-absorption potential, as over IGP airborne particles are predominately fine and strongly UV-absorbing while across SEA, fine and UV-neutral aerosols prevail.

3.3. Trend in Aerosol Properties in Urban Hotspots

Nonparametric trend in monthly mean AOD and other aerosol time series for individual sites are presented in Figure 6 with 95% level of confidence included in Table S4. In Kumar et al. (2018), we quantified the

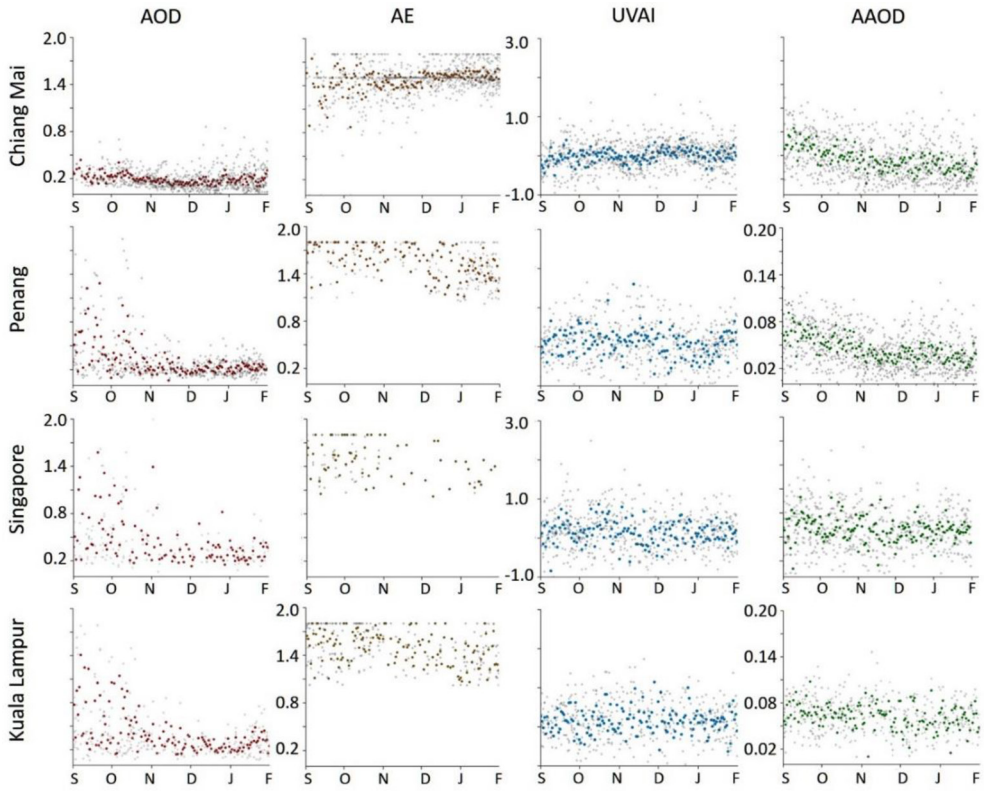

Figure 5. Time series of aerosol optical and microphysical properties in different urban hotspots across SEA. *Note*: Gray dots indicate daily retrievals while mean averaged over 2010–2020 is indicated in color dot. To manage a similar scale for intercomparison, <2% of extreme observations were excluded. All the individual parameter bears identical scale (S, September; O, October; N, November; D, December; J, January; F, February). SEA, Southeast Asia.

long-term geospatial trend in AOD across IGP (0.002 years^{-1}) which was spatially inconsistent, having only robust and significant increasing trend over central to lower IGP. Here, for the haze dominating period (October-February), all the mainland sites in IGP denote spatially consistent and an increasing trend in AOD, varying from 0.937×10^{-2} year^{-1} (Varanasi) to 1.06×10^{-2} year^{-1} (Lahore). A minor increasing trend in AOD across IGP is in accordance to the previously reported observation both by Kumar et al. (2018) using satellite (Terra-MODIS; 2006–2015) and Khan et al. (2019) using AERONET database (2001–2018). Interestingly, annual trend in AOD is negative in Dhaka (-2.40×10^{-3} year^{-1}) and is comparable to the continental site Chiang Mai in northern Thailand (-2.03×10^{-3} year^{-1}). This emphasize the resemblance of these two sites in terms of aerosol source profile as both are possibly influenced by the local emission sources. Other SEA sites experience an increasing trend in AOD (0.2–1.8×10^{-2} year^{-1}) indicating influence of the transported biomass burning emissions from Indonesia and southern Malaysia.

Decadal trend in AE is declining across all the cities with trivial spatial variation except in Karachi, which experiences a statistically significant decreasing trend (-9.62×10^{-2} year^{-1}) during haze period. The most interesting feature in Figure 6 is to identify the robust increase in UV-absorbing aerosols for all the sites across IGP and SEA. Indeed, all the sites over upper IGP record high and statistically significant increasing trend in UVAI varying from 2.86×10^{-2} year^{-1} (Delhi) to 6.02×10^{-2} year^{-1} (Lahore). Rest of the cities in IGP also record an increase in UVAI in the last decade but the rate declines gradually among the cities from upper to lower IGP. Among SEA cities, Kuala Lumpur (2.63×10^{-2} year^{-1}) experiences the highest increasing trend in UVAI followed by Singapore (1.28×10^{-2} year^{-1}), both possibly associated with rapid urbanization and associated emission sources. Decadal trend in AAOD is however low except for Lahore (4.72×10^{-3} year^{-1}). Overall, nonparametric trend analysis of aerosol loading and aerosol columnar properties typically indicate systematic increase in aerosol loading and absorbing aerosols over IGP (except in

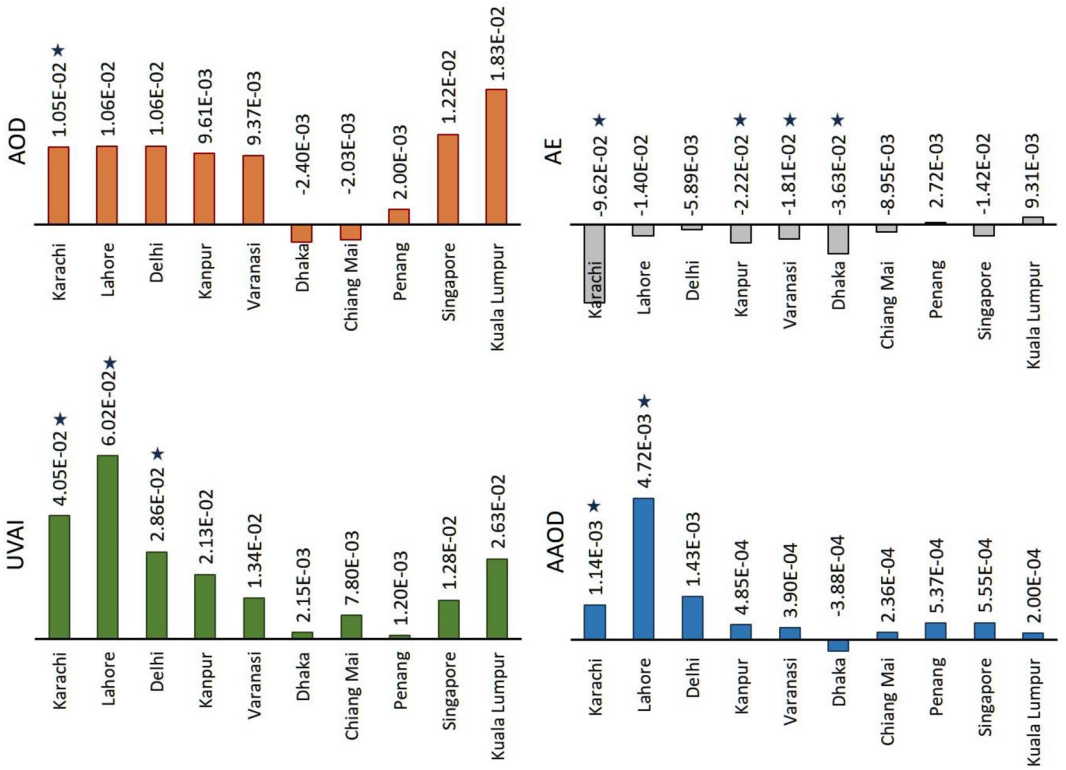

Figure 6. Trend in aerosol properties (year^{-1}) in different urban hotspots. *Note*: A * indicate statistically significant change.

Dhaka) and maritime countries over SEA during typical haze dominating period which requires further investigation in terms of their sources and implications, both in regional climate and human health.

3.4. Classification of Existing Aerosol Types

Aerosols over individual sites were classified constraining AE and UVAI, and predominate aerosols during haze period is shown in Figure 7 and in Table S5. Among the nine aerosol classes, absorbing coarse (AC) was treated as mineral dust aerosols as being largely nonspherical particles with high UV-absorption potential mainly due to the presence of iron oxide. Both AM and AF types indicate carbonaceous smoke aerosols of biomass burning, vehicular and industrial origin which are primarily small to medium sized particles with high UV-absorbing potential (Vadrevu et al., 2014; Vinjamuri et al., 2020). However, there are evidences that UVAI may decrease with corresponding decline in aerosol layer height, reduction in AOD and with increase cloudiness (Penning de Vries et al., 2015). This instigates us to also consider NF aerosol type to signify smoke aerosols, especially over the SEA which accounts greater cloudiness and lower aerosol layer height. In contrast, scattering aerosols of finer size (SF) bears signal of biogenic aerosols while coarse aerosols (SC) indicate marine aerosols. Following this classification scheme, a total of four dominating aerosol types were assigned: smoke (AM, AF, and NF); mineral dust (AC); marine (SC), and biogenic aerosols (SF).

During October-February, presence of mineral dust (46%) is only traced in Karachi with rest of the days mostly bearing signature of smoke particle abundance. For the rest of the cities across IGP, AF particles clearly dominates (59–81%), highest over the cities in upper IGP (Lahore: 76%; Delhi: 81%) with gradual decline toward central to lower IGP. Overall, smoke particles contribute 85% (Dhaka) to 98% (Delhi) of haze days during October to February months across IGP, 71–91% of days particularly with highly UV-absorbing aerosols, thereby having potential to largely influence regional radiation balance. Indeed, smoke particles also dominate over the SEA cities, accounting 84–92% of retrieval days. However, in contrast to IGP, NF aerosols dominates over all the SEA cities (51–61%) except in Singapore which experiences an even distribution

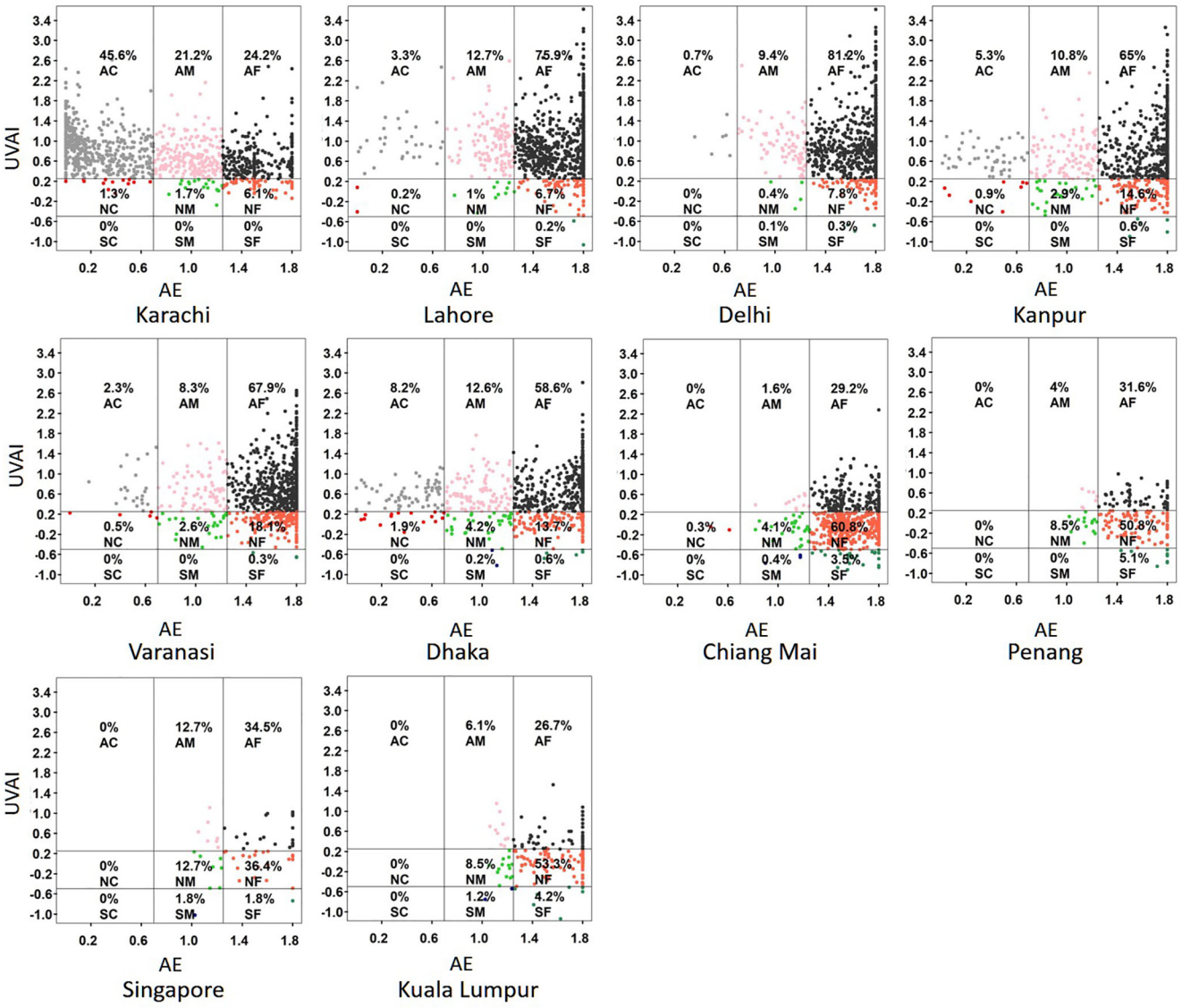

Figure 7. Predominating aerosol types during typical haze conditions in different cities across South and Southeast Asia. *Note*: Aerosol types color-coded according to size and absorption. The first character in aerosol types represents the optical properties, i.e., A, Absorbing; N, Neutral; and S, Scattering; and the second character represents size, i.e., F, Fine; M, Mixed; and C, Coarse. For example, AF represent Absorbing Fine aerosol type.

of UV-neutral to absorbing aerosols (AF: 35%; NF: 36%). Interestingly, marine aerosols (SC) does not dominate among none of the cities while dominance of biogenic aerosols (SF) is only traced over SEA cities.

3.5. Vertical Distribution of Aerosols

Aerosol extinction coefficient during haze dominated period in between 2010 and 2020 was retrieved over individual sites (1° × 1°) across IGP and SEA. We followed latest and improved CALIPSO version 4.20 aerosol profile which has many improvements against its predecessor, and has better aerosol retrieval accuracy over south Asia (Kim et al., 2018). Following the outcome of existing aerosol types over urban hotspots (in Figure 7), aerosol types having highest extinction at surface level are only included in Figure 8 while profiles of mean aerosol extinction for all CALISPO aerosol types are shown in Figure S2. To classify existing aerosol type based on ratio of extinction to backscattering at 532 nm; smoke aerosols (biomass burning and associated aerosols) were identified for an aggregate lidar ratio of 70 ± 25 sr (for polluted continental/smoke) and 70 ± 16 sr (for elevated smoke), while dust aerosol was retrieved at 44 ± 9 sr. Another aerosol type, polluted

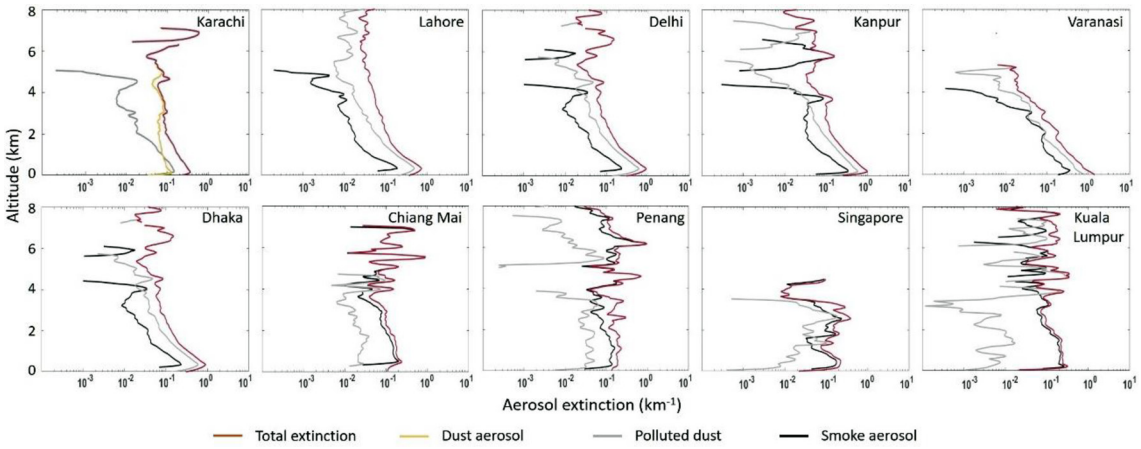

Figure 8. Vertical profiles of mean extinction coefficient of predominating aerosols over different urban hotspots.

dust (55 ± 22 sr), essentially a mixture of AERONET desert dust (coarse mode) and biomass burning (fine mode) clusters was retrieved, signifying urban aerosols with a mixture of dust and biomass burning smoke aerosols (Kim et al., 2018; Omar et al., 2009). We also hypothesized insignificant spatial variations within the defined space among the sites.

3.5.1. Vertical Distribution of Aerosol Extinction

Vertical distribution (<8 km) of aerosol extinction coefficient across two geographical regions, as shown in Figure 8, indicates two striking features: first, a gradual decline in aerosol extinction with height is only prominent for the cities over IGP; second, clearly polluted dust and smoke dominate the existing aerosol type. Likewise, for every urban hotspot across IGP, vertical gradient in total aerosol extinction is negative, more pronounce over Varanasi and lowest in Karachi. A relatively high extinction at surface level denotes the greater contribution of local sources compared to the transported one. Among the sites in IGP, the maximum near surface (<1 km) total aerosol extinction is retrieved in Varanasi (1.4 km^{-1}), following minimum discrepancies among Dhaka, Kanpur, Delhi, and Lahore (~1 km^{-1}); while total surface aerosol extinction is lowest in Karachi (0.3 km^{-1}). All the IGP sites resemble in having polluted dust as the most dominating aerosol type with highest extinction at surface (<1 km). Polluted dust bears the signature of typical urban aerosols, with sources associated to biomass burning, crustal resuspensions, and other anthropogenic emissions. Smoke aerosols which are typical carbonaceous aerosols induce the second highest extinction at surface in all the IGP sites except in Karachi while its contribution to total aerosol extinction increases gradually from upper to lower IGP. A characteristic peak in smoke extinction close to 4 km vertical height is also noted, possibly influenced by transported aerosols, as also evident by Kumar et al. (2015, 2017) during typical winter months.

Vertical profiles of dust aerosol extinction yield interesting result (Figure S2). For all the IGP sites, dust extinction does not vary significantly with height and its contribution to total aerosol extinction amplifies with increasing height. Karachi remains the solitary site that experiences significant extinction attribute by dust aerosols near surface (<1 km) and in between 3-km and 5-km height. Total aerosol extinction remains almost stable with height over Karachi with an apparent zone of aerosol accumulation at 6–7 km. A similar zone of aerosol accumulation was also noted over Delhi, Kanpur, and Dhaka at 6–8-km height. Overall, dust remains a significant contributor to total aerosol extinction for all the sites over upper IGP (Karachi, Lahore, and Delhi); while over central IGP (Kanpur and Varanasi) polluted dust dominates, and over lower IGP (Dhaka), both smoke and polluted dust mainly contribute to total aerosol extinction. However, it is worth to mention that CALIPSO detects dust based on discrete dipole approximation considering realistic composition and irregular shapes of particle (Kalashnikova & Sokolik, 2002). So, it is quite possible for CALIPSO to miss approximate or overestimate moisture-laden finer particle as coarser dust due to its hygroscopic growth.

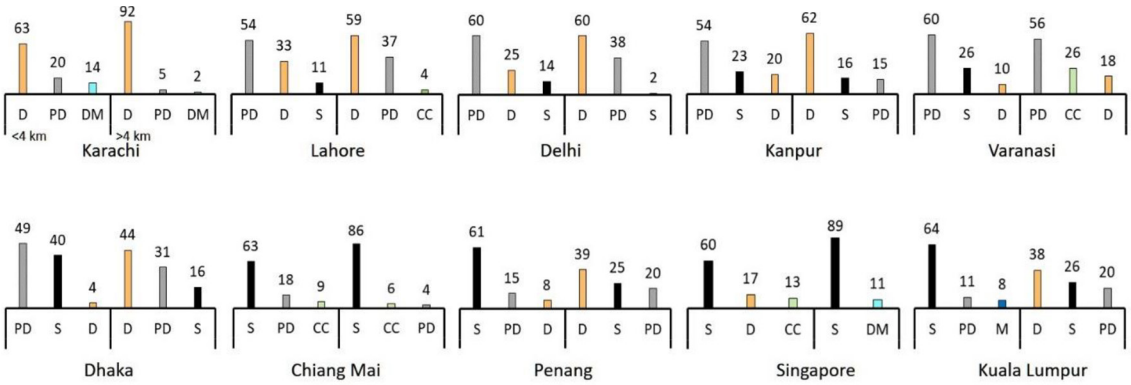

Figure 9. Relative abundance (in %) of predominating aerosol types over different urban hotspots across South and Southeast Asia. *Note*: Left column indicates a vertical height of <4 km from surface and right-side panel indicates vertical height of >4 km and beyond. D, dust; PD, polluted dust; DM, dusty marine; S, smoke; CC, clean continental; M, marine.

All the SEA sites denote comparatively low vertical gradient in total aerosol extinction implying robust contribution from transported aerosols across the atmospheric column. However, variations in individual aerosol extinction with increasing height is common for all the sites bearing the influence of Trade wind with greater velocity compared to the slow blowing westerly over South Asia (Figure S3). Figure S3 indicates, there is an intrusion of ocean surface wind over upper IGP during September except which wind blowing over IGP is continental westerly. In comparison, wind blowing over SEA is both from Bay of Bengal (in September) and South China Sea (October-January) with relatively higher wind speed. There is a clear dominance of biomass burning smoke aerosols across all the SEA sites at surface; that contributes chiefly to total aerosol extinction up to 4 km vertical height, followed by the polluted dust. However, marine aerosol also found to contribute at surface (<800 m) both over Singapore and Kuala Lumpur before diminishing with increasing height. Besides, an intrusion of dust aerosols with extinction varying from 0.03 to 0.10 km^{-1} at a vertical height >6 km is detected over Penang and Kuala Lumpur which may possibly be the wind-blown dust of transboundary origin.

3.5.2. Relative Abundance of Aerosol Types

Relative abundance of aerosol types during haze dominating period for each urban hotspot over South and Southeast Asia are plotted in Figure 9. Although not exhaustive, these aerosol subtypes provide valuable information on the distribution of aerosols across the atmospheric column, from surface to layer top height as detected by CALISPO over individual station. Considering a strong gradient in the distribution of aerosol species relative to its height, vertical distribution of aerosol subtype was made for two scenarios: first, from surface to vertical height up to 4 km (<4 km) and second, the upper atmosphere for a vertical height beyond 4 km (>4 km). Such classification of atmospheric profile yields interesting results as in the lower atmosphere (<4 km), polluted dust (PD) clearly dominates the aerosol subtype across the IGP except in Karachi. Relative abundance of polluted dust varies from 49% (Dhaka) to 60% (Delhi, Varanasi) with the lowest in Karachi (20%). Dust aerosols (D) abundance gradually diminishes from upper IGP (25–63%) to central IGP (10–20%) before being the lowest over lower IGP (4%). This is in contrast to the smoke aerosols (S) as its abundance increases consistently from upper (11–14%) to central IGP (23–26%) before reaching to its maximum over lower IGP (40%). At upper atmosphere (>4 km), however, dust aerosols dominate aerosol profile across IGP varying from 44% to 92% with the lowest abundance over Varanasi (18%) followed by Dhaka (44%). This clearly establish the spatial gradient in existing aerosol types that prevails across the atmospheric column over IGP during haze dominating period which possibly have diverse implications on regional health-climate-agriculture system. In contrast, a clear dominance of smoke aerosols is depicted across the Southeast Asia both at lower (60–64%) and in upper atmosphere (25–89%) followed by polluted dust aerosol (11–18%).

We conclude from the CALIPSO observations that during haze dominating period, both the IGP and SEA bear the similar character in having prevalence of smoke aerosols. However, over IGP, vertical gradient in aerosol distribution is especially evident as in lower atmosphere; smoke aerosols are more mixed with urban

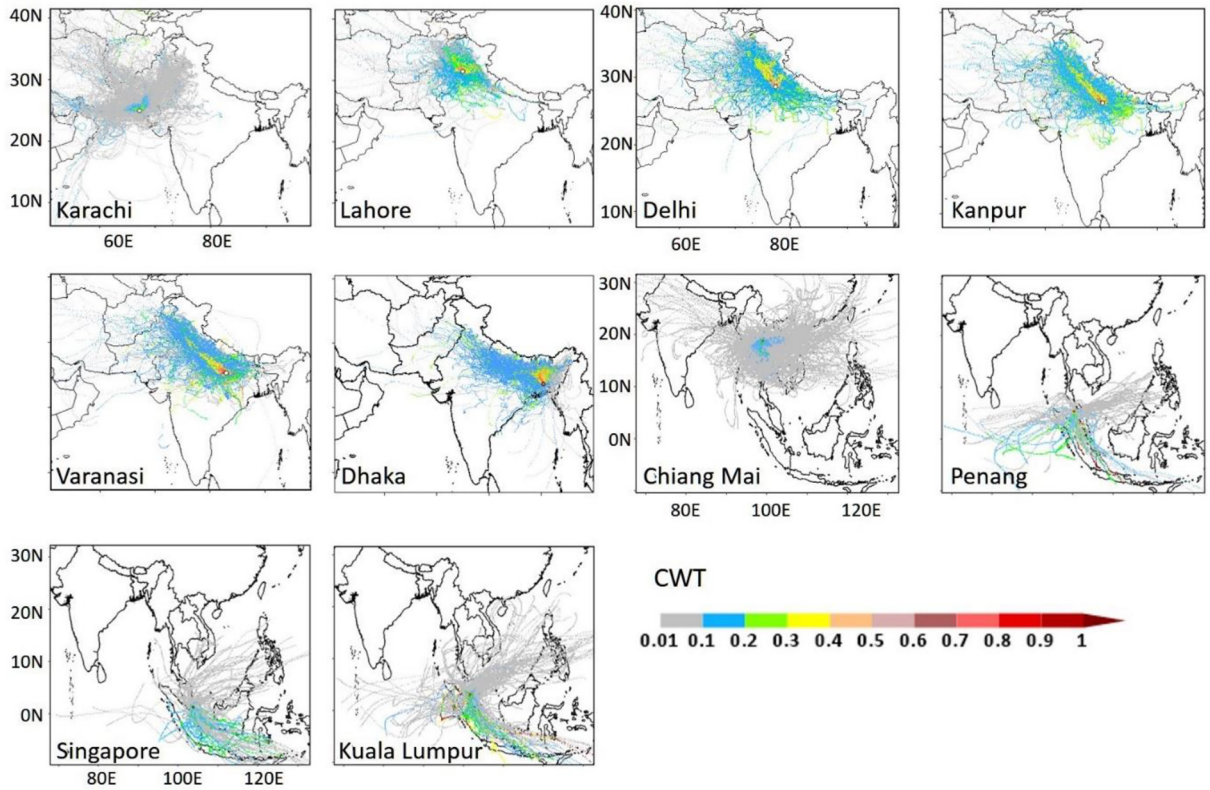

Figure 10. Aerosols potential source filed during haze dominating period. *Note*: CWTs (unitless) were plotted only for haze dominating period in between 2018 and 2019 for sites over IGP (at 500 and 1,500 m) and SEA (at 1,500, 1,900, and 2,300 m). CWTs, Concentration weighted trajectories; IGP, Indo-Gangetic plain; SEA, Southeast Asia.

aerosols with typical sources like anthropogenic emissions and remains close to the surface compared to SEA, where smoke aerosols are more evenly distributed across the atmospheric column. In contrast, at upper atmosphere, a clear dominance of dust aerosols is noted over upper IGP which gradually subside toward lower IGP with subsequent increase in polluted dust and smoke aerosols. This also reestablish our previous report in Vinjamuri et al. (2020) that over smoke dominated region in upper IGP, although smoke travels efficiently beyond planetary boundary layer to free troposphere but it remains close to the surface (<3 km) which may have greater implications to human exposure and regional climate.

3.6. Aerosol Potential Source Fields

To assess the possible source fields and intracontinental transport of airborne particulates across South and Southeast Asia, 5-days concentration weighted trajectories (CWTs) were drawn in Figure 10. The CWTs were plotted for all the urban hotspots accounting prevailing mean average planetary boundary layer height as reported in Murari et al. (2017) and McGrath-Spangler and Denning (2013).

Indeed, Karachi receives aerosols transported by air masses both from ocean and continental origin. For the cities across IGP, except Karachi, all receive robust contribution from continental westerlies with very few trajectories originated from ocean. Likewise, for Lahore, potential high aerosol source regions are close to the city, with major contribution from western dry regions of Sulaiman range, Thal desert and from upper IGP. The CWTs for Delhi, Kanpur, and Varanasi resembles by having moderate to high contributions (CWT > 0.3) from sources located over western semiarid regions, including northern parts of Pakistan and Punjab (India). However, these cities also pose potential source field over central highlands and lower Gangetic plain, but their overall contribution are relatively low (CWT < 0.2). This concludes that during postmonsoon to winter, continental westerlies originating from upper IGP and western semiarid regions predominately contribute high to very high columnar aerosol loading in cities across the IGP (Kumar

et al., 2017, 2018; Murari et al., 2020). Potential aerosol source field for Dhaka, however, slightly differs with moderate to high CWTs (>0.4) originating mainly from central Bangladesh with added contribution by westerly blowing across IGP. This essentially establish that columnar air quality over Dhaka primarily receives pollution from local sources which resulted a slight deviation in existing aerosol properties compared to inland cities.

Continental and maritime air masses are seen over the cities across SEA, however, none originating from IGP except few for Chiang Mai with very low CWTs. Chiang Mai receives aerosol laden air masses from across Thailand, western Cambodia and from eastern part of Burma, all with low CWTs (<0.1) but probably it receives the major proportion of aerosols from southern Thailand. Interestingly, biomass burning emission from Kalimantan and Sumatra is not found to reach till Chiang Mai which is more prominent for the rest of the SEA cities. Indeed, Penang, Singapore, and Kuala Lumpur has similar aerosol source fields. Besides receiving maritime air masses from South China sea and Andaman Sea; all the maritime cities receive air masses from Riau province of Sumatra (and southern Malaysia) which has been reported to account for major proportion of Southeast Asian forest and peat land burning emissions (Vadrevu et al., 2014). Intra-periodic variations in aerosol source fields were also explored for the sites over SEA (Figure S4). Clearly, higher CWTs during September-October are originated from the southern Malaysia, Indonesia and from Kalimantan while CWTs during November-January are contributing less to regional aerosol loading.

4. Conclusions

Aerosol climatology over two globally recognized hotspots, South Asia and Southeast Asia (SEA), was explored for the haze dominating period in between 2010 and 2020. Several satellite-based aerosol optical properties were retrieved using coordinated Earth-Observing A-Train satellites (sensor) like Aqua (MODIS), Aura (OMI), and CALIPSO (CALIOP). Indeed, the Indo-Gangetic plain (IGP) bears the highest columnar aerosol loading (AOD) within South Asia, much higher than the aerosol loading over SEA. Besides, prevailing aerosols are finer in size but with robust variations in UV-absorption potential; as much of the aerosols across IGP are highly UV-absorbing compared to UV-neutral aerosols over SEA. Presence of UV-absorbing fine aerosols is detected in close proximity to its reported source locations, especially over the upper IGP, east Indonesia, and southern part of Malaysia.

Daily variations in aerosol properties over urban pollution hotspots yield interesting results. Abundance of coarse particles is only noted in Karachi while the rest of the cities like Lahore, Delhi, Kanpur, and Varanasi exhibit a single peak in UVAI (>1.3) during November and a bimodal distribution in AOD, with the first peak in early November followed by in early January. Daily time series clearly indicate a transition in aerosol loading and optical properties in cities across IGP which is not evident over SEA. Rather all the cities over SEA (except Chiang Mai) denote typical September-October peak in aerosol loading with prevalence of UV-neutral aerosols. A spatially consistent and minor increasing decadal trend in AOD is noted for most of the cities over IGP and SEA (except Dhaka and Chiang Mai), while a statistically significant increase in UVAI only in Karachi, Lahore, and in Delhi, all located over the upper IGP.

Aerosol classification scheme revealed the dominance of dust aerosols only in Karachi (46%) while absorbing fine particles with signature of smoke aerosols prevails over Lahore, Delhi, Kanpur, Varanasi, and in Dhaka (71–91%). Indeed, smoke particles are dominant over SEA cities, however, with less UV-absorbing potentials. CALIPSO lidar profiles further validate the predominating aerosol types and establish vertical distribution of aerosols. Vertical stratification of aerosols is particularly evident over the IGP as in lower atmosphere, polluted dust/urban aerosols dominate across the region with consequent decrease in relative abundance of dust from upper to lower IGP and corresponding increase in smoke aerosols. This was in contrast to SEA where clear dominance of smoke aerosols is noted across the vertical atmospheric column followed by polluted dust and dust aerosols. Potential aerosol source fields across urban hotspots were also simulated. We do not found evidence of intracontinental transport of aerosols from IGP to Southeast Asia or vice versa.

Conflict of Interest

The authors declare no conflicts of interest relevant to this study.

Data Availability Statement

MODIS data are available at https://ladsweb.modaps.eosdis.nasa.gov. Aura-OMI data are available from https://earthdata.nasa.gov. CALIPSO data are available from the NASA Atmospheric Science Data Center (https://eosweb.larc.nasa.gov). ERA-Interim Archive is available on the ECMWF website (http://ecmwf.int/en/research/climate-reanalysis/era-interim). All data sets were last accessed in April 2020.

Acknowledgments
The research was financially supported by the ASEAN-India Science and Technology Development Fund, Govt. of India under ASEAN-India Collaborative Research and Development Scheme (CRD/2018/000011). T. Banerjee also acknowledges funds received from University Grants Commission under India-Israel bilateral research project (6-11/2018 IC). Authors are thankful to anonymous reviewers for their constructive comments and suggestions.

References

Ahn, C., Torres, O., & Jethva, H. (2014). Assessment of OMI near-UV aerosol optical depth over land. *Journal of Geophysical Research: Atmospheres*, *119*, 2457–2473. https://doi.org/10.1002/2013JD020188

Begum, B., Kim, E., Biswas, S. K., & Hopke, P. K. (2004). Investigation of sources of atmospheric aerosol at urban and semi-urban areas in Bangladesh. *Atmospheric Environment*, *38*, 3025–3038. https://doi.org/10.1016/j.atmosenv.2004.02.042

Bilal, M., & Nichol, J. E. (2015). Evaluation of MODIS aerosol retrieval algorithms over the Beijing-Tianjin-Hebei region during low to very high pollution events. *Journal of Geophysical Research: Atmospheres*, *120*, 7941–7957. https://doi.org/10.1002/2015JD023082

Bilal, M., Nichol, J. E., & Nazeer, M. (2016). Validation of Aqua-MODIS C051 and C006 operational aerosol products using AERONET measurements over Pakistan. *IEEE Journal of Selected Topics in Applied Earth Observations Remote Sensing*, *9*(5), 2074–2080. https://doi.org/10.1109/jstars.2015.2481460

Bollasina, M. A., Ming, Y. & Ramaswamy, V. (2011). Anthropogenic aerosols and the weakening of the South Asian summer monsoon. *Science*, *334*, 502–505. https://doi.org/10.1126/science.1204994

Bourgeois, Q., Ekman, A. M. L., Renard, J.-B., Krejci, R., Devasthale, A., Bender, F. A.-M., et al. (2018). How much of the global aerosol optical depth is found in the boundary layer and free troposphere? *Atmospheric Chemistry and Physics*, *18*, 7709–7720. https://doi.org/10.5194/acp-18-7709-2018

Chakraborty, A., Bhattu, D., Gupta, T., Tripathi, S. N. & Canagaratna, M. R. (2015). Real-time measurements of ambient aerosols in a polluted Indian city: Sources, characteristics, and processing of organic aerosols during foggy and nonfoggy periods. *Journal of Geophysical Research: Atmospheres*, *120*, 9006–9019. https://doi.org/10.1002/2015JD023419

Cohen, J. B. (2014). Quantifying the occurrence and magnitude of the Southeast Asian fire climatology. *Environmental Research Letters*, *9*(11), 114018. https://doi.org/10.1088/1748-9326/9/11/114018

Dey, S., & Di Girolamo, L. (2011). A decade of change in aerosol properties over the Indian subcontinent. *Geophysical Research Letters*, *38*, L14811. https://doi.org/10.1029/2011GL048153

Dey, S., Tripathi, S. N. & Mishra, S. K. (2008). Probable mixing state of aerosols in the Indo-Gangetic Basin, northern India. *Geophysical Research Letters*, *35*, L03808. https://doi.org/10.1029/2007GL032622

Duncan, B. N., Bey, I., Chin, M., Mickley, L. J., Fairlie, T. D., Martin, R. V., & Matsueda, H. (2003). Indonesian wildfires of 1997: Impact on tropospheric chemistry. *Journal of Geophysical Research*, *108*(D15), 4458. https://doi.org/10.1029/2002JD003195

Field, R. D., Van Der Werf, G. R., & Shen, S. S. P. (2009). Human amplification of drought-induced biomass burning in Indonesia since 1960. *Nature Geoscience*, *2*(3), 185–188. https://doi.org/10.1038/ngeo443

Gautam, R., Hsu, N. C., Tsay, S. C., Lau, K. M., Holben, B., Bell, S., et al. (2011). Accumulation of aerosols over the Indo-Gangetic plains and southern slopes of the Himalayas: Distribution, properties and radiative effects during the 2009 pre-monsoon season. *Atmospheric Chemistry and Physics*, *11*(24), 12841–12863. https://doi.org/10.5194/acp-11-12841-2011

Henriksson, S. V., Laaksonen, A., Kerminen, V.-M., Räisänen, P., Järvinen, H., Sundström, A.-M., & de Leeuw, G. (2011). Spatial distributions and seasonal cycles of aerosols in India and China seen in global climate-aerosol model. *Atmospheric Chemistry and Physics*, *11*(15), 7975–7990. https://doi.org/10.5194/acp-11-7975-2011

Herman, J. R., Bhartia, P. K., Torres, O., Hsu, C., Seftor, C., & Celarier, E. (1997). Global distribution of UV-absorbing aerosols from Nimbus 7/TOMS data. *Journal of Geophysical Research*, *102*, 16911–16922. https://doi.org/10.1029/96JD03680

Huijnen, V., Wooster, M. J., Kaiser, J. W., Gaveau, D. L., Flemming, J., Parrington, M., et al. (2016). Fire carbon emissions over maritime Southeast Asia in 2015 largest since 1997. *Scientific Reports*, *6*, 26886. https://doi.org/10.1038/srep26886

Jain, S., Sharma, S. K., Vijayan, N. & Mandal, T. K. (2020). Seasonal characteristics of aerosols (PM2. 5 and PM10) and their source apportionment using PMF: A four year study over Delhi, India. *Environmental Pollution*, *262*, 114337.

Jeong, M. J., & Li, Z. (2005). Quality, compatibility, and synergy analyses of global aerosol products derived from the advanced very high resolution radiometer and Total Ozone Mapping Spectrometer. *Journal of Geophysical Research*, *110*, D10S08. https://doi.org/10.1029/2004JD004647

Jethva, H., Satheesh, S. K., & Srinivasan, J. (2005). Seasonal variability of aerosols over the Indo-Gangetic basin. *Journal of Geophysical Research*, *110*, D21204. https://doi.org/10.1029/2005JD005938

Jethva, H., Torres, O., & Ahn, C. (2014). Global assessment of OMI aerosol single-scattering albedo using ground-based AERONET inversion. *Journal of Geophysical Research: Atmospheres*, *119*, 9020–9040. https://doi.org/10.1002/2014JD021672

Jethva, H., Torres, O., & Ahn, C. (2018). A 12-year long global record of optical depth of absorbing aerosols above the clouds derived from the OMI/OMACA algorithm. *Atmospheric Measurement Techniques*, *11*, 5837–5864. https://doi.org/10.5194/amt-11-5837-2018

Jethva, H., Torres, O., Field, R. D., Lyapustin, A., Gautam, R., & Kayetha, V. (2019). Connecting crop productivity, residue fires, and air quality over northern India. *Scientific Reports*, *9*(1), 16594. https://doi.org/10.1038/s41598-019-52799-x

Kalashnikova, O. V., & Sokolik, I. N., (2002). Importance of shapes and compositions of wind-blown dust particles for remote sensing at solar wavelengths. *Geophysical Research Letters*, *29*(10), 1398. https://doi.org/10.1029/2002GL014947

Khan, R., Kumar, K. R., & Zhao, T. (2019). The climatology of aerosol optical thickness and radiative effects in Southeast Asia from 18-years of ground-based observations. *Environmental Pollution*, *254*, 113025. https://doi.org/10.1016/j.envpol.2019.113025

Kim, J., Lee, J., Lee, H. C., Higurashi, A., Takemura, T., & Song, C. H. (2007). Consistency of the aerosol type classification from satellite remote sensing during the Atmospheric Brown Cloud–East Asia Regional Experiment campaign. *Journal of Geophysical Research*, *112*, D22S33. https://doi.org/10.1029/2006JD008201

Kim, M.-H., Omar, A. H., Tackett, J. L., Vaughan, M. A., Winker, D. M., Trepte, C. R., et al. (2018). The CALIPSO version 4 automated aerosol classification and lidar ratio selection algorithm. *Atmospheric Measurement Techniques*, *11*, 6107–6135. https://doi.org/10.5194/amt-11-6107-2018

Klimont, Z., Kupiainen, K., Heyes, C., Purohit, P., Cofala, J., Rafaj, P., et al. (2017). Global anthropogenic emissions of particulate matter including black carbon. *Atmospheric Chemistry and Physics*, *17*(14), 8681–8723. https://doi.org/10.5194/acp-17-8681-2017

Krishna Moorthy, K., Suresh Babu, S., Manoj, M. R., & Satheesh, S. K. (2013). Buildup of aerosols over the Indian Region. *Geophysical Research Letters*, *40*, 1011–1014. https://doi.org/10.1002/grl.50165

Kumar, M., Parmar, K. S., Kumar, D. B., Mhawish, A., Broday, D. M., Mall, R. K. & Banerjee, T. (2018). Long-term aerosol climatology over Indo-Gangetic Plain: Trend, prediction and potential source fields. *Atmospheric Environment*, *180*, 37–50. https://doi.org/10.1016/j.atmosenv.2018.02.027

Kumar, M., Raju, M. P., Singh, R. K., Singh, A. K., Singh, R. S., & Banerjee, T. (2017). Wintertime characteristics of aerosols over middle Indo-Gangetic Plain: Vertical profile, transport and radiative forcing. *Atmospheric Research*, *183*, 268–282. https://doi.org/10.1016/j.atmosres.2016.09.012

Kumar, M., Tiwari, S., Murari, V., Singh, A. K., & Banerjee, T. (2015). Wintertime characteristics of aerosols at middle Indo-Gangetic Plain: Impacts of regional meteorology and long range transport. *Atmospheric Environment*, *104*, 162–175. https://doi.org/10.1016/j.atmosenv.2015.01.014

Latif, M. T., Othman, M., Idris, N., Juneng, L., Abdullah, A. M., Hamzah, W. P., et al. (2018). Impact of regional haze towards air quality in Malaysia: A review. *Atmospheric Environment*, *177*, 28–44. https://doi.org/10.1016/j.atmosenv.2018.01.002

Lee, J., Kim, J., Song, C. H., Kim, S. B., Chun, Y., Sohn, B. J., & Holben, B. N. (2010). Characteristics of aerosol types from AERONET sunphotometer measurements. *Atmospheric Environment*, *44*(26), 3110–3117. https://doi.org/10.1016/j.atmosenv.2010.05.035

Li, J., Carlson, B. E., Dubovik, O., & Lacis, A. A. (2014). Recent trends in aerosol optical properties derived from AERONET measurements. *Atmospheric Chemistry and Physics*, *14*(22), 12271–12289. https://doi.org/10.5194/acp-14-12271-2014

Lyapustin, A., Wang, Y., Laszlo, I., Kahn, R., Korkin, S., Remer, L., et al. (2011). Multiangle implementation of atmospheric correction (MAIAC): 2. Aerosol algorithm. *Journal of Geophysical Research*, *116*, D03211. https://doi.org/10.1029/2010JD014986

Mansha, M., Ghauri, B., Rahman, S., & Amman, A. (2012). Characterization and source apportionment of ambient air particulate matter (PM2.5) in Karachi. *Science of the Total Environment*, *425*, 176–183. https://doi.org/10.1016/j.scitotenv.2011.10.056

McGrath-Spangler, E. L. & Denning, A. S. (2013). Global seasonal variations of midday planetary boundary layer depth from CALIPSO space-borne LIDAR. *Journal of Geophysical Research: Atmospheres*, *118*, 1226–1233. https://doi.org/10.1002/jgrd.50198

Mhawish, A., Banerjee, T., Broday, D. M., Misra, A., & Tripathi, S. N. (2017). Evaluation of MODIS Collection 6 aerosol retrieval algorithms over Indo-Gangetic Plain: Implications of aerosols types and mass loading. *Remote Sensing of Environment*, *201*, 297–313. https://doi.org/10.1016/j.rse.2017.09.016

Mhawish, A., Banerjee, T., Sorek-Hamer, M., Bilal, M., Lyapustin, A. I., Chatfield, R., & Broday, D. M. (2020). Estimation of high-resolution PM2.5 over the Indo-Gangetic Plain by fusion of satellite data, meteorology, and land use variables. *Environmental Science and Technology*, *54*(13), 7891–7900. https://dx.doi.org/10.1021/acs.est.0c01769

Mhawish, A., Banerjee, T., Sorek-Hamer, M., Lyapustin, A., Broday, D. M., & Chatfield, R. (2019). Comparison and evaluation of MODIS Multi-angle Implementation of Atmospheric Correction (MAIAC) aerosol product over South Asia. *Remote Sensing of Environment*, *224*, 12–28. https://doi.org/10.1016/j.rse.2019.01.033

Murari, V., Kumar, M., Mhawish, A., Barman, S. C. & Banerjee, T. (2017). Airborne particulate in Varanasi over middle Indo-Gangetic Plain: Variation in particulate types and meteorological influences. *Environmental Monitoring and Assessment*, *189*, 157. https://doi.org/10.1007/s10661-017-5859-9

Murari, V., Singh, N., Ranjan, R., Singh, R. S., & Banerjee, T. (2020). Source apportionment and health risk assessment of airborne particulates over central Indo-Gangetic Plain. *Chemosphere*, *257*, 127145.

Nguyen, T. T., Pham, H. V., Lasko, K., Bui, M. T., Laffly, D., Jourdan, A., & Bui, H. Q. (2019). Spatiotemporal analysis of ground and satellite-based aerosol for air quality assessment in the Southeast Asia region. *Environmental Pollution*, *255*, 113106. https://doi.org/10.1016/j.envpol.2019.113106

Ojha, N., Sharma, A., Kumar, M., Girach, I., Ansari, T. U., Sharma, S. K., et al. (2020). On the widespread enhancement in fine particulate matter across the Indo-Gangetic Plain towards winter. *Scientific Reports*, *10*(1), 5862. https://doi.org/10.1038/s41598-020-62710-8

Omar, A. H., Winker, D. M., Vaughan, M. A., Hu, Y., Trepte, C. R., Ferrare, R. A., et al. (2009). The CALIPSO automated aerosol classification and lidar ratio selection algorithm. *Journal of Atmospheric and Oceanic Technology*, *26*, 1994–2014. https://doi.org/10.1175/2009jtecha1231.1

Penning de Vries, M. J. M., Beirle, S., Hörmann, C., Kaiser, J. W., Stammes, P., Tilstra, L. G., et al. (2015). A global aerosol classification algorithm incorporating multiple satellite data sets of aerosol and trace gas abundances. *Atmospheric Chemistry and Physics*, *15*(18), 10597–10618. https://doi.org/10.5194/acp-15-10597-2015

Quah, E., & Johnston, D. (2001). Forest fires and environmental haze in Southeast Asia: Using the 'stakeholder' approach to assign costs and responsibilities. *Journal of Environmental Management*, *63*, 181–191. https://doi.org/10.1006/jema.2001.0475

Rajput, P., & Sarin, M. M. (2014). Polar and non-polar organic aerosols from large-scale agricultural-waste burning emissions in Northern India: Implications to organic mass-to-organic carbon ratio. *Chemosphere*, *103*, 74–79. https://doi.org/10.1016/j.chemosphere.2013.11.028

Ramanathan, V., Crutzen, P. J., Kiehl, J. T., & Rosenfeld, D. (2001). Aerosols, climate, and the hydrological cycle. *Science*, *294*, 2119–2124. https://doi.org/10.1126/science.1064034

Sahani, M., Zainon, N. A., Wan Mahiyuddin, W. R., Latif, M. T., Hod, R., Khan, M. F., et al. (2014). A case-crossover analysis of forest fire haze events and mortality in Malaysia. *Atmospheric Environment*, *96*, 257–265. https://doi.org/10.1016/j.atmosenv.2014.07.043

Sayer, A. M., Hsu, N. C., Lee, J., Kim, W. V., & Dutcher, S. T. (2019). Validation, stability, and consistency of MODIS Collection 6.1 and VIIRS Version 1 Deep Blue aerosol data over land. *Journal of Geophysical Research: Atmospheres*, *124*, 4658–4688. https://doi.org/10.1029/2018JD029598

Shi, Y., Matsunaga, T., Yamaguchi, Y., Li, Z., Gu, X., & Chen, X. (2018). Long-term trends and spatial patterns of satellite-retrieved PM2.5 concentrations in South and Southeast Asia from 1999 to 2014. *Science of the Total Environment*, *615*, 177–186. https://doi.org/10.1016/j.scitotenv.2017.09.241

Singh, N., Banerjee, T., Murari, V., Deboudt, K., Khan, F., Singh, R. S. & Latif, T. (2021). Insights into size-segregated particulate chemistry and sources in urban environment over central Indo-Gangetic Plain. *Chemosphere*, *263*, 128030. https://doi.org/10.1016/j.chemosphere.2020.128030

Singh, N., Banerjee, T., Raju, M. P., Deboudt, K., Sorek-Hamer, M., Singh, R. S. & Mall, R. K. (2018). Aerosol chemistry, transport, and climatic implications during extreme biomass burning emissions over the Indo-Gangetic Plain. *Atmospheric Chemistry and Physics*, *18*(19), 14197–14215. https://doi.org/10.5194/acp-18-14197-2018

Singh, N., Mhawish, A., Banerjee, T., Ghosh, S., Singh, R. S. & Mall, R. (2021). Air pollution induced mortality in an urban pollution hotspot over central Indo-Gangetic Plain. *Atmospheric Environment*, *246*, 118088. https://doi.org/10.1016/j.atmosenv.2020.118088

Singh, N., Mhawish, A., Deboudt, K., Singh, R. S., & Banerjee, T. (2017). Organic aerosols over Indo-Gangetic Plain: Sources, distributions and climatic implications. *Atmospheric Environment*, *157*, 59–74. https://doi.org/10.1016/j.atmosenv.2017.03.008

Singh, N., Murari, V., Kumar, M., Barman, S. C., & Banerjee, T. (2017). Fine particulates over South Asia: Review and meta-analysis of PM2.5 source apportionment through receptor model. *Environmental Pollution*, *223*, 121–136. https://doi.org/10.1016/j.envpol.2016.12.071

Sonkar, G., Mall, R. K., Banerjee, T., Singh, N., Kumar, T. V. L., & Chand, R. (2019). Vulnerability of Indian wheat against rising temperature and aerosols. *Environmental Pollution*, *254*, 112946. https://doi.org/10.1016/j.envpol.2019.07.114

Srivastava, R. (2017). Trends in aerosol optical properties over South Asia. *International Journal of Climatology*, *37*(1), 371–380. https://doi.org/10.1002/joc.4710

Stockwell, C. E., Jayarathne, T., Cochrane, M. A., Ryan, K. C., Putra, E. I., Saharjo, B. H., et al. (2016). Field measurements of trace gases and aerosols emitted by peat fires in Central Kalimantan, Indonesia, during the 2015 El Niño. *Atmospheric Chemistry and Physics*, *16*(2016), 11711–21173. https://doi.org/10.5194/acp-16-11711-2016

Stone, E., Schauer, J., Quraishi, T. A., & Mahmood, A. (2010). Chemical characterization and source apportionment of fine and coarse particulate matter in Lahore, Pakistan. *Atmospheric Environment*, *44*, 1062–1070. https://doi.org/10.1016/j.atmosenv.2009.12.015

Sulong, N. A., Latif, M. T., Khan, M. F., Amil, N., Ashfold, M. J., Wahab, M. I. A., et al. (2017). Source apportionment and health risk assessment among specific age groups during haze and non-haze episodes in Kuala Lumpur, Malaysia. *Science of the Total Environment*, *601–602*, 556–570. https://doi.org/10.1016/j.scitotenv.2017.05.153

Thomas, A., Sarangi, C., & Kanawade, V. P. (2019). Recent increase in Winter Hazy Days over central India and the Arabian Sea. *Scientific Reports*, *9*(1), 17406. https://doi.org/10.1038/s41598-019-53630-3

Torres, O., Tanskanen, A., Veihelmann, B., Ahn, C., Braak, R., Bhartia, P. K., et al. (2007). Aerosols and surface UV products from Ozone Monitoring Instrument observations: An overview. *Journal of Geophysical Research*, *112*, D24S47. https://doi.org/10.1029/2007JD008809

Turetsky, M. R., Benscoter, B., Page, S., Rein, G., van der Werf, G. R., & Watts, A. (2015). Global vulnerability of peatlands to fire and carbon loss. *Nature Geoscience*, *8*, 11–14. https://doi.org/10.1038/ngeo2325

Vadrevu, K. P., Lasko, K., Giglio, L., & Justice, C. (2014). Analysis of Southeast Asian pollution episode during June 2013 using satellite remote sensing datasets. *Environmental Pollution*, *195*, 245–256. https://doi.org/10.1016/j.envpol.2014.06.017

Vadrevu, K. P., Lasko, K., Giglio, L., Schroeder, W., Biswas, S., & Justice, C. (2019). Trends in vegetation fires in South and Southeast Asian countries. *Scientific Reports*, *9*(1), 7422. https://doi.org/10.1038/s41598-019-43940-x

Vinjamuri, K. S., Mhawish, A., Banerjee, T., Sorek-Hamer, M., Broday, D. M., Mall, R. K., & Latif, M. T. (2020). Vertical distribution of smoke aerosols over upper Indo-Gangetic Plain. *Environmental Pollution*, *257*, 113377. https://doi.org/10.1016/j.envpol.2019.113377

Vinoj, V., Rasch, P. J., Wang, H., Yoon, J.-H., Ma, P.-L., Landu, K., & Singh, B. (2014). Short-term modulation of Indian summer monsoon rainfall by West Asian dust. *Nature Geoscience*, *7*(4), 308–313. https://doi.org/10.1038/ngeo2107

Wang, Y. Q., Zhang, X. Y. & Draxler, R. R. (2009). TrajStat: GIS-based software that uses various trajectory statistical analysis methods to identify potential sources from long-term air pollution measurement data. *Environmental Modelling and Software*, *24*(8), 938–939. https://doi.org/10.1016/j.envsoft.2009.01.004

Winker, D. M., Vaughan, M. A., Omar, A., Hu, Y., Powell, K. A., Liu, Z., et al. (2009). Overview of the CALIPSO mission and CALIOP data processing algorithms. *Journal of Atmospheric and Oceanic Technology*, *26*, 2310–2323. https://doi.org/10.1175/2009jtecha1281.1

Yanhong, T., Naoki, K., Akio, F., & Awang, M. (1996). Light reduction by regional haze and its effect on simulated leaf photosynthesis in a tropical forest of Malaysia. *Forest Ecology and Management*, *89*, 205–211. https://doi.org/10.1016/s0378-1127(96)03849-2

Yin, S., Wang, X., Zhang, X., Guo, M., Miura, M., & Xiao, Y. (2019). Influence of biomass burning on local air pollution in mainland Southeast Asia from 2001 to 2016. *Environmental Pollution*, *254*, 112949. https://doi.org/10.1016/j.envpol.2019.07.117